Inorg. Chem. **2005**, *44*, 6219–6227

Syntheses, Structures, and Luminescent and Magnetic Properties of Novel Three-Dimensional Lanthanide Complexes with 1,3,5-Benzenetriacetate

Zheng-Hua Zhang,[†] Taka-aki Okamura,[‡] Yasuchika Hasegawa,[§] Hiroyuki Kawaguchi,[||] Ling-Yan Kong,[†] Wei-Yin Sun,*[,†] and Norikazu Ueyama[‡]

Coordination Chemistry Institute, State Key Laboratory of Coordination Chemistry, Nanjing University, Nanjing 210093, China, Department of Macromolecular Science, Graduate School of Science, Osaka University, Toyonaka, Osaka 560-0043, Japan, Material and Life Science, Graduate School of Engineering, Osaka University, Suita 565-0871, Japan, and Coordination Chemistry Laboratories, Institute for Molecular Science, Okazaki, Aichi 444-8585, Japan

Received March 25, 2005

Five novel lanthanide complexes with the formulas $[Nd(bta)(H_2O)_2 \cdot 4.35H_2O]_n$ (**1**), $[Sm(bta)(H_2O)_2 \cdot 4.5H_2O]_n$ (**2**), $[Eu(bta)(H_2O) \cdot 1.48H_2O]_n$ (**3**), $[Tb(bta)(H_2O) \cdot 1.31H_2O]_n$ (**4**), and $[Yb(bta)(H_2O) \cdot H_2O]_n$ (**5**) (H_3bta = 1,3,5-benzenetriacetic acid) have been prepared by using the corresponding lanthanide salt and H_3bta. The results of an X-ray crystallographic analysis revealed that all the complexes have three-dimensional channel-like structures, in which the bta^{3-} ligands adopt different coordination modes: monodentate and μ_2-η^2:η^1-bridging coordination modes in **1**, **2**, and **5** and μ_2-η^1:η^1-bridging and μ_2-η^2:η^1-bridging coordination modes in **3** and **4**, respectively. Complexes **1** and **2**, as well as **3** and **4**, are isostructural, respectively, in which all the Ln^{III} (Ln = Nd, Sm, Eu, and Tb) atoms are nine-coordinated, while the Yb^{III} atoms in complex **5** are eight-coordinated. Both complexes **3** and **4** showed strong luminescence upon excitation, and their luminescence decay curves fit well with single exponential decays of which the lifetime is 0.45 ms for **3** and 1.0 ms for **4**. The magnetic properties of the complexes were investigated in the temperature range of 1.8–300 K.

Introduction

The constructions and characterizations of inorganic−organic hybrid materials based on transition metal carboxylates are of continuous interests because of their unusual topologies and relevance in a wide range of applications in material science including superconductors, magnetic materials, catalysts, and luminescent materials.[1] However, in recent years, there has been an upsurge in the use of lanthanide salts for constructing such kinds of materials. Because of the unique nature of lanthanide ions, such as their large radius, high and variable coordination numbers, and the existence of multi−single electrons, the assembly of lanthanide complexes with novel structures and specific properties offers great challenges and opportunities in terms of controlling their shape and dimensionality.[2] A great number of three-dimensional (3D) lanthanide polymeric complexes with multicarboxylate ligands have been reported,[3] which indicates that a careful choice of organic ligands coupled with the lanthanide ions can lead to the formation of new complexes with interesting structures and unique properties. Recent studies concerning the use of 1,3,5-benzenetriacetic acid (H_3bta) as a ligand toward alkaline-earth and transition metal salts have shown that a great variety of polymeric structures can be obtained as a result of the different

* To whom correspondence should be addressed. E-mail: sunwy@nju.edu.cn. Fax: 86-25-83314502.
[†] Nanjing University, China.
[‡] Graduate School of Science, Osaka University, Japan.
[§] Graduate School of Engineering, Osaka University, Japan.
[||] Institute for Molecular Science, Japan.

(1) (a) Kim, Y. J.; Jung, D.-Y. *Inorg. Chem.* **2000**, *39*, 1470. (b) Cheng, D.; Khan, M. A.; Houser, R. P. *Inorg. Chem.* **2001**, *40*, 6858. (c) Lee, E. W.; Kim, Y. J.; Jung, D.-Y. *Inorg. Chem.* **2002**, *41*, 501. (d) Konar, S.; Mukherjee, P. S.; Drew, M. G. B.; Ribas, J.; Chaudhuri, N. R. *Inorg. Chem.* **2003**, *42*, 2545. (e) Choi, H. J.; Suh, M. P. *J. Am. Chem. Soc.* **2004**, *126*, 15844. (f) Lin, Z.; Jiang, F.; Chen, L.; Yuan, D.; Hong, M. *Inorg. Chem.* **2005**, *44*, 73.

(2) (a) Tsukube, H.; Shinoda, S. *Chem. Rev.* **2002**, *102*, 2389. (b) Ghosh, S. K.; Bharadwaj, P. K. *Inorg. Chem.* **2003**, *42*, 8250. (c) Li, X.; Shi, Q.; Sun, D.; Bi, W.; Cao, R. *Eur. J. Inorg. Chem.* **2004**, 2747. (d) Su, C.-Y.; Smith, M. D.; Goforth, A. M.; Loye, H.-C. Z. *Inorg. Chem.* **2004**, *43*, 6881. (e) Thirumurugan, A.; Natarajan, S. *J. Chem. Soc., Dalton Trans.* **2004**, 2923.

10.1021/ic050453a CCC: $30.25
Published on Web 08/11/2005

conformation and coordination modes of the bta^{3-} ligand.[4] The previous work has proved that H_3bta is a good building block for the construction of lanthanide polymers, and several open frameworks have been obtained by hydro/solvothermal reactions of H_3bta with light lanthanide ions.[5] The successful isolation of these complexes prompted us to carry out the assembly of other lanthanide salts with H_3bta to build new coordination polymers. Herein, we report the preparation, X-ray crystal structures, photoluminescent properties, and magnetic study of five novel lanthanide coordination polymers—$[Nd(bta)(H_2O)_2 \cdot 4.35H_2O]_n$ (**1**), $[Sm(bta)(H_2O)_2 \cdot 4.5H_2O]_n$ (**2**), $[Eu(bta)(H_2O) \cdot 1.48H_2O]_n$ (**3**), $[Tb(bta)(H_2O) \cdot 1.31H_2O]_n$ (**4**), and $[Yb(bta)(H_2O) \cdot H_2O]_n$ (**5**).

Experimental Section

Materials and Measurements. All commercially available solvents and starting materials were used as received without further purification. The H_3bta ligand was prepared by the method described in the literature.[6] Hydrated lanthanide nitrates were prepared from the corresponding oxides according to the literature methods.[7] Elemental analyses were taken on a Perkin−Elmer 240C elemental analyzer, at the Analysis Center of Nanjing University. FT-IR spectra were recorded on a Bruker Vector22 FT-IR spectrophotometer in KBr disks. Thermogravimetric and differential thermal analyses were performed on a simultaneous SDT 2960 thermal analyzer. Powder samples were loaded into alumina pans and heated from room temperature to 800 °C under N_2 at a heating rate of 10 °C/min. The luminescent spectra of the solid samples were acquired at ambient temperature by using a JOBIN YVON/HORIBA SPEX Fluorolog t3 system (slit: 0.1 nm). The spectra were corrected for the detector sensitivity and lamp intensity variations. Emission lifetimes were measured using an SPEX Fluorolog t3 system (slit: 0.5 nm) with a SPEX phosphorimeter 1934D (flush lamp pulse: 0.04 ms). The temperature-dependent magnetic susceptibilities in the temperature range of 1.8−300 K under a constant external magnetic field of 2000 G were performed on an MPMS−SQUID magnetometer. The diamagnetic contributions of the samples were corrected by using Pascal's constants.

Preparation of the Complexes. $[Nd(bta)(H_2O)_2 \cdot 4.35H_2O]_n$ (1). An aqueous solution of tetra-*tert*-butylammonium salt of H_3bta was readily prepared by the reaction of tetra-*tert*-butylammonium hydroxide (*t*-Bu_4NOH) with H_3bta in aqueous solution until the pH was 7. The title complex **1** was prepared by slow diffusion between two layers of an aqueous solution (10 mL) of the tetra-*tert*-butylammonium salt of H_3bta (0.1 mmol) and $NdCl_3 \cdot 6H_2O$ (0.0358 g, 0.1 mmol) in ethanol (10 mL) at room temperature. About 1 week later, single crystals suitable for X-ray analysis were obtained in 70% yield. Anal. Calcd for $C_{12}H_{21.69}NdO_{12.35}$: C, 28.38; H, 4.31%. Found: C, 28.51; H, 4.49%. IR (KBr, cm^{-1}): 3423 (br), 1637 (m), 1610 (m), 1543 (vs), 1428 (s), 1419 (s), 1395 (vs), 1273 (s), 1172 (w), 1046 (w), 742 (m), 625 (m). The TGA data for **1** show that the initial weight loss of 21.73% occurred from 50 to 310 °C, which corresponds well with the loss of all water molecules (including coordinated and uncoordinated water molecules, calculated: 22.49%); the second weight loss begins at 405 °C, where the decomposition starts.

$[Sm(bta)(H_2O)_2 \cdot 4.5H_2O]_n$ (2). The complex was prepared by the same method described for complex **1** using $SmCl_3 \cdot 6H_2O$ (0.0365 g, 0.1 mmol) instead of $NdCl_3 \cdot 6H_2O$. Yield: 70%. Anal. Calcd for $C_{12}H_{22}O_{12.50}Sm$: C, 27.90; H, 4.29%. Found: C, 27.75; H, 4.16%. IR (KBr, cm^{-1}): 3419 (br), 1637 (m), 1610 (m), 1546 (vs), 1429 (s), 1417 (s), 1395 (vs), 1274 (s), 1173 (w), 1046 (w), 743 (m), 626 (m). The TGA data for **2** show that the initial weight loss occurred from 40 to 310 °C, corresponding to the loss of all water molecules; the second weight loss begins at 410 °C, where the decomposition of the residue starts.

$[Eu(bta)(H_2O) \cdot 1.48H_2O]_n$ (3). The complex was prepared by a solvothermal method. A mixture of $Eu(NO_3)_3 \cdot 6H_2O$ (0.0446 g, 0.1 mmol), H_3bta (0.0252 g, 0.1 mmol), C_2H_5OH (2 mL), and H_2O (10 mL) was stirred for about 15 min at room temperature. Then, the mixture was transferred and kept in a Teflon-lined autoclave at 160 °C for 3 days. After the mixture was cooled to room temperature over 12 h, colorless block crystals of **3** were obtained. Yield: 78%. Anal. Calcd for $C_{12}H_{13.96}O_{8.48}Eu$: C, 32.33; H, 3.16%. Found: C, 32.19; H, 3.13%. IR (KBr, cm^{-1}): 3560 (m), 3374 (br), 1639 (m), 1590 (s), 1549 (vs), 1445 (s), 1418 (vs), 1305 (m), 1279 (m), 1174 (w), 775 (m), 643 (s). The TGA data for **3** show that the initial weight loss of 10.69% occurred from 60 to 140 °C, which corresponds well with the loss of all water molecules (calculated: 10.01%); the second weight loss begins at 380 °C, where the decomposition starts.

$[Tb(bta)(H_2O) \cdot 1.31H_2O]_n$ (4). The complex was prepared by the same method described for complex **3** using $Tb(NO_3)_3 \cdot 6H_2O$ (0.0453 g, 0.1 mmol) instead of $Eu(NO_3)_3 \cdot 6H_2O$. Yield: 74%. Anal. Calcd for $C_{12}H_{13.62}O_{8.31}Tb$: C, 32.05; H, 3.05%. Found: C, 31.95; H, 3.04%. IR (KBr, cm^{-1}): 3559 (m), 3374 (br), 1640 (m), 1594 (s), 1551 (vs), 1445 (s), 1420 (vs), 1307 (m), 1279 (w), 1174 (m), 777 (m), 643 (s). The TGA data of **4** show that the first weight loss of 9.02% occurring from 65 to 145 °C corresponds to the loss of all water molecules (calculated: 9.25%), and the further loss was not observed before 450 °C, where the decomposition starts.

$[Yb(bta)(H_2O) \cdot H_2O]_n$ (5). The title complex was synthesized by a hydrothermal reaction. A mixture of $Yb(NO_3)_3 \cdot 6H_2O$ (0.0467 g, 0.1 mmol), H_3bta (0.0252 g, 0.1 mmol), and H_2O (12 mL) was sealed in a stainless steel vessel and placed in an oven, then directly heated to 160 °C and kept for 3 days. After the mixture was cooled to room temperature over 12 h, colorless platelet crystals of **5** were obtained in 70% yield. Anal. Calcd for $C_{12}H_{13}O_8Yb$: C, 31.45; H, 2.86%. Found: C, 31.38; H, 2.77%. IR (KBr, cm^{-1}): 3535 (m), 3239 (s), 1636 (m), 1591 (vs), 1560 (vs), 1427 (vs), 1406 (vs), 1264 (s), 1170 (w), 747 (m), 613 (m). The TGA data of **5** show that the initial weight loss of 7.35% begins at 65 °C and ends at 175 °C, which corresponds to the loss of all water molecules (calculated: 7.85%), and then, the decomposition of the residue starts at 415 °C.

Crystallographic Analyses. The collections of crystallographic data were carried out on a Rigaku Mercury CCD area detector at

(3) (a) Reineke, T. M.; Eddaoudi, M.; O'Keeffe, M.; Yaghi, O. M. *Angew. Chem., Int. Ed.* **1999**, *38*, 2590. (b) Reineke, T. M.; Eddaoudi, M.; Fehr, M.; Kelley, D.; Yaghi, O. M. *J. Am. Chem. Soc.* **1999**, *121*, 1651. (c) Eddaoudi, M.; Kim, J.; Wachter, J. B.; Chae, H. K.; O'Keeffe, M.; Yaghi, O. M. *J. Am. Chem. Soc.* **2001**, *123*, 4368. (d) Pan, L.; Woodlock, E. B.; Wang, X. *Inorg. Chem.* **2000**, *39*, 4174. (e) Cao, R.; Sun, D. F.; Liang, Y. C.; Hong, M. C.; Tataumi, K.; Shi, Q. *Inorg. Chem.* **2002**, *41*, 2087. (f) Paz, F. A. A.; Klinowski, J. *Chem. Commun.* **2003**, 1484. (g) Costes, J. P.; Juan, J. M. C.; Dahan, F.; Nicodème, F. *J. Chem. Soc., Dalton Trans.* **2003**, 1272. (h) Hernández-Molina, M.; Ruiz-Pérez, C.; López, T.; Lloret, F.; Julve, M. *Inorg. Chem.* **2003**, *42*, 5456. (g) Zheng, X.-J.; Wang, Z.-M.; Gao, S.; Liao, F.-H.; Yan, C.-H.; Jin, L.-P. *Eur. J. Inorg. Chem.* **2004**, 2968.

(4) (a) Zhu, H.-F.; Sun, W.-Y.; Okamura, T.-a.; Ueyama, N. *Inorg. Chem. Commun.* **2003**, *6*, 168. (b) Zhu, H.-F.; Zhang, Z.-H.; Sun, W.-Y.; Okamura, T.-a.; Ueyama, N. *Cryst. Growth Des.* **2005**, *5*, 177.

(5) Zhang, Z.-H.; Shen, Z.-L.; Okamura, T.-a.; Zhu, H.-F.; Sun, W.-Y.; Ueyama, N. *Cryst. Growth Des.* **2005**, *5*, 1191.

(6) Newman, M. S.; Lowrie, H. S. *J. Am. Chem. Soc.* **1954**, *76*, 6196.

(7) Bünzli, J. C. G.; Chopin, G. R. *Lanthanide Probes in Life, Chemical and Earth Sciences*; Elsevier: Amsterdam, 1989.

Table 1. Crystallographic Data for Complexes **1**−**5**

complex	**1**	**2**	**3**	**4**	**5**
chemical formula	$C_{12}H_{21.69}NdO_{12.35}$	$C_{12}H_{22}O_{12.50}Sm$	$C_{12}H_{13.96}O_{8.48}Eu$	$C_{12}H_{13.62}O_{8.31}Tb$	$C_{12}H_{13}O_8Yb$
fw	507.77	516.65	445.86	449.43	458.26
crystal system	triclinic	triclinic	triclinic	triclinic	triclinic
space group	$P\bar{1}$	$P\bar{1}$	$P\bar{1}$	$P\bar{1}$	$P\bar{1}$
a, Å	8.4735(7)	8.4310(11)	7.727(2)	7.673(3)	6.044(6)
b, Å	10.8836(9)	10.841(2)	9.705(3)	9.661(3)	10.780(10)
c, Å	11.1301(2)	11.114 00(10)	10.580(3)	10.533(4)	11.486(10)
α, deg	64.333(19)	64.43(4)	106.61(3)	106.54(3)	68.71(7)
β, deg	80.33(3)	80.44(6)	105.28(3)	105.28(3)	75.01(8)
γ, deg	73.76(2)	73.82(5)	100.69(3)	100.62(3)	87.61(6)
V, Å^3	886.93(19)	878.8(4)	703.7(4)	693.0(4)	672.4(10)
Z	2	2	2	2	2
T, K	173	173	200	200	200
μ (Mo Kα), mm^{-1}	2.988	3.404	4.497	5.142	6.991
D_{calcd}, g cm^{-3}	1.901	1.953	2.104	2.154	2.263
λ, Å	0.710 70	0.710 70	0.710 75	0.710 75	0.710 75
R_{int}	0.028	0.041	0.0519	0.0432	0.0675
$R[I > 2\sigma(I)]^a$	0.0456	0.1189	0.0261	0.0245	0.0826
$wR[I > 2\sigma(I)]^b$	0.1227	0.2969	0.0551	0.0537	0.2253

^{a} $R = \sum||F_o| - |F_c||/\sum|F_o|$. ^{b} $wR = |\sum w(|F_o|^2 - |F_c|^2)|/\sum|w(F_o)^2|^{1/2}$, where $w = 1/[\sigma^2(F_o^2) + (aP)^2 + bP]$. $P = (F_o^2 + 2F_c^2)/3$.

173 K for complexes **1** and **2** and on a Rigaku RAXIS−RAPID Imaging Plate diffractometer at 200 K for complexes **3**−**5**, using graphite monochromated Mo Kα radiation (λ = 0.7107 Å). The structures were solved by direct methods with SIR92[8] and expanded using Fourier techniques.[9] All data for non-hydrogen atoms were refined anisotropically by the full-matrix least-squares method. The hydrogen atoms were generated geometrically except for those of the water molecules. All calculations were carried out on an SGI workstation using the teXsan crystallographic software package of the Molecular Structure Corporation.[10] Details of the crystal parameters, data collection, and refinement for complexes **1**−**5** are summarized in Table 1. Selected bond lengths and angles with their estimated standard deviations are listed in Table 2. Further details are provided in the Supporting Information.

Results and Discussions

Preparation of the Complexes. The coordination chemistry of H_3bta with transition metals has been studied in recent years,[4a] and our aim is to investigate the coordination chemistry of Ln-bta (Ln is a lanthanide metal), and we hope to obtain novel complexes with specific structures and properties as well as to investigate the effect of the lanthanide contraction on the structure of the complexes. Five complexes with three kinds of structures were successfully isolated by using different synthetic techniques.

When *t*-Bu_4NOH was employed to neutralize the H_3bta, complexes **1** and **2** were obtained in satisfying yields by the layering method. While other kinds of bases, for example, pyridine, piperidine, NaOH, Na_2CO_3, K_2CO_3, $NaHCO_3$, or $Mg(OH)_2$, were used to neutralize the H_3bta, unfortunately, no single crystals were obtained. In addition, the hydro(solvo)thermal method has been extensively used in the preparation of highly stable, infinite-coordination polymers. The reactions of H_3bta with varied lanthanide salts were carried out under hydro(solvo)thermal conditions, and the results showed that only the complexes with lanthanide metals heavier than the samarium could be obtained by hydro(solvo)thermal reactions. The different results between the layering and hydro(solvo)thermal reactions may be caused by a different reaction mechanism.[11]

Description of Crystal Structures. $[Nd(bta)(H_2O)_2\cdot 4.35H_2O]_n$ (1) and $[Sm(bta)(H_2O)_2\cdot 4.5H_2O]_n$ (2). Complexes **1** and **2** are isomorphous and isostructural, and they have a similar structure to that of the reported complex $[La(bta)(H_2O)_2]\cdot 4.5H_2O$.[5] For example, in complex **2**, the Sm^{III} center is nine-coordinated by seven O atoms from five different bta^{3-} ligands and from two ones from two coordinated water molecules (Figure 1a), and each bta^{3-} ligand adopts a cis, trans, trans conformation and acts as a μ_5-bridge to link five metal atoms (Scheme 1a), in which one carboxylate group adopts a monodentate mode coordinating to one samarium atom while each of the other two carboxylate groups adopts a μ_2-η^2:η^1-bridging (namely, one O atom of the carboxylate connects two metal atoms, the other one connects one metal atom, and the carboxylate group coordinates to two metal atoms) coordination mode connecting two samarium atoms. If we neglect the linkage of the monodentate carboxylate groups in bta^{3-}, a two-dimensional (2D) network is obtained (Figure 1b). In this network, the Sm^{III} atoms and μ_2-η^2:η^1-bridging O atoms form an infinite one-dimensional (1D) Sm−O chain, and in each chain, the Sm^{III} atoms are almost in a straight line (∠Sm1B−Sm1J−Sm1K = ∠Sm1J−Sm1K−Sm1R = 177.1°), and then, the bridged bta^{3-} ligands link these 1D chains to generate a ladder-like 2D network (Figure 1b). The 2D networks are further linked together by the monodentate carboxylate groups to give a 3D channel-like coordination polymer (Figure 1c), and the uncoordinated water molecules are trapped in the channels of the 3D framework (Figure S1 in the Supporting Information).

(8) SIR92: Altomare, A.; Burla, M. C.; Camalli, M.; Cascarano, M.; Giacovazzo, C.; Guagliardi, A.; Polidori, G. *J. Appl. Cryst*. **1994**, *27*, 435.

(9) DIRFID 94: Beurskens, P. T.; Admiraal, G.; Beurskens, G.; Bosman, W. P.; de Gelder, R.; Israel, R.; Smits, J. M. M. *The DIRFID-94 Program System*; Technical Reportof the Crystallography Laboratory; University of Nijmegen: Nijmegen, The Netherlands, 1994.

(10) *teXsan*; Molecular Structure Corporation: The Woodlands, TX, 1999.

(11) (a) Bemazeau, G. *J. Mater. Chem*. **1999**, *9*, 15. (b) Feng, S. H.; Xu, R. R. *Acc. Chem. Res*. **2001**, *34*, 239.

Table 2. Selected Bond Distances (Å) and Angles (deg) for **1**−**5**

1[a]

Nd−O(1)	2.552(4)	Nd−O(1)#1	2.459(4)	Nd−O(2)	2.570(4)
Nd−O(3)	2.524(4)	Nd−O(4)	2.626(4)	Nd−O(4)#2	2.409(4)
Nd−O(5)	2.351(5)	Nd−O(7)	2.474(4)	Nd−O(8)	2.524(5)
O(1)−Nd−O(1)#1	64.48(16)	O(1)−Nd−O(2)	50.86(14)	O(1)−Nd−O(3)	118.75(14)
O(1)−Nd−O(4)	155.02(15)	O(1)−Nd−O(4)#2	122.34(13)	O(1)−Nd−O(5)	82.55(18)
O(1)−Nd−O(7)	72.85(15)	O(1)−Nd−O(8)	133.24(16)	O(1)#1−Nd−O(2)	114.83(14)
O(1)#1−Nd−O(3)	71.35(14)	O(1)#1−Nd−O(4)	119.30(13)	O(1)#1−Nd−O(4)#2	156.17(16)
O(1)#1−Nd−O(5)	108.4(2)	O(1)#1−Nd−O(7)	79.96(15)	O(1)#1−Nd−O(8)	82.84(16)
O(2)−Nd−O(3)	145.91(18)	O(2)−Nd−O(4)	122.42(14)	O(2)−Nd−O(4)#2	73.30(15)
O(2)−Nd−O(5)	73.04(19)	O(2)−Nd−O(7)	75.05(17)	O(2)−Nd−O(8)	136.31(17)
O(3)−Nd−O(4)	50.30(13)	O(3)−Nd−O(4)#2	115.42(14)	O(3)−Nd−O(5)	73.3(2)
O(3)−Nd−O(7)	137.32(17)	O(3)−Nd−O(8)	76.44(17)	O(4)−Nd−O(4)#2	65.42(16)
O(4)−Nd−O(5)	72.81(17)	O(4)−Nd−O(7)	131.47(15)	O(4)−Nd−O(8)	70.05(16)
O(4)#2−Nd−O(5)	95.4(2)	O(4)#2−Nd−O(7)	80.90(15)	O(4)#2−Nd−O(8)	77.13(17)
O(5)−Nd−O(7)	147.56(18)	O(5)−Nd−O(8)	141.83(19)	O(7)−Nd−O(8)	69.06(16)

2[b]

Sm−O(1)	2.614(12)	Sm−O(1)#1	2.382(12)	Sm−O(2)	2.515(15)
Sm−O(3)	2.419(11)	Sm−O(4)	2.549(11)	Sm−O(4)#2	2.414(11)
Sm−O(5)	2.308(17)	Sm−O(7)	2.447(13)	Sm−O(8)	2.502(14)
O(1)−Sm−O(1)#1	64.6(5)	O(1)−Sm−O(2)	50.4(4)	O(1)−Sm−O(3)	118.1(4)
O(1)−Sm−O(4)	154.5(4)	O(1)−Sm−O(4)#2	120.1(4)	O(1)−Sm−O(5)	73.8(5)
O(1)−Sm−O(7)	131.4(4)	O(1)−Sm−O(8)	69.9(5)	O(1)#1−Sm−O(2)	114.7(5)
O(1)#1−Sm−O(3)	62.3(4)	O(1)#1−Sm−O(4)	123.2(4)	O(1)#1−Sm−O(4)#2	155.9(4)
O(1)#1−Sm−O(5)	96.3(6)	O(1)#1−Sm−O(7)	81.5(5)	O(1)#1−Sm−O(8)	76.9(5)
O(2)−Sm−O(3)	155.8(5)	O(2)−Sm−O(4)	118.5(4)	O(2)−Sm−O(4)#2	72.1(4)
O(2)−Sm−O(5)	73.6(6)	O(2)−Sm−O(7)	136.9(5)	O(2)−Sm−O(8)	75.9(5)
O(3)−Sm−O(4)	61.1(4)	O(3)−Sm−O(4)#2	121.4(4)	O(3)−Sm−O(5)	82.7(5)
O(3)−Sm−O(7)	67.3(4)	O(3)−Sm−O(8)	123.2(4)	O(4)−Sm−O(4)#2	64.0(4)
O(4)−Sm−O(5)	81.1(5)	O(4)−Sm−O(7)	73.5(4)	O(4)−Sm−O(8)	133.8(4)
O(4)#2−Sm−O(5)	107.8(6)	O(4)#2−Sm−O(7)	79.1(4)	O(4)#2−Sm−O(8)	82.9(4)
O(5)−Sm−O(7)	147.3(6)	O(5)−Sm−O(8)	142.3(6)	O(7)−Sm−O(8)	69.2(5)

3[c]

Eu−O(1)	2.456(3)	Eu−O(2)	2.372(3)	Eu−O(2)#2	2.571(3)
Eu−O(3)	2.451(3)	Eu−O(4)	2.370(3)	Eu−O(5)	2.492(3)
Eu−O(6)	2.485(3)	Eu−O(6)#1	2.503(3)	Eu−O(7)	2.447(3)
O(1)−Eu−O(2)	122.73(9)	O(1)−Eu−O(2)#2	51.53(9)	O(1)−Eu−O(3)	100.59(11)
O(1)−Eu−O(4)	78.00(10)	O(1)−Eu−O(5)	143.67(11)	O(1)−Eu−O(6)	75.93(9)
O(1)−Eu−O(6)#1	139.29(8)	O(1)−Eu−O(7)	77.32(10)	O(2)−Eu−O(2)#2	72.40(10)
O(2)−Eu−O(3)	71.08(10)	O(2)−Eu−O(4)	74.23(10)	O(2)−Eu−O(5)	74.09(10)
O(2)−Eu−O(6)	141.10(10)	O(2)−Eu−O(6)#2	96.38(9)	O(2)−Eu−O(7)	141.47(10)
O(2)#2−Eu−O(3)	74.40(10)	O(2)#2−Eu−O(4)	71.87(9)	O(2)#2−Eu−O(5)	138.92(8)
O(2)#2−Eu−O(6)#1	154.52(10)	O(2)#2−Eu−O(6)	108.65(9)	O(2)#2−Eu−O(7)	124.88(10)
O(3)−Eu−O(4)	137.25(9)	O(3)−Eu−O(5)	115.68(11)	O(3)−Eu−O(6)	72.00(9)
O(3)−Eu−O(6)#1	80.35(10)	O(3)−Eu−O(7)	142.59(9)	O(4)−Eu−O(5)	76.72(9)
O(4)−Eu−O(6)	144.30(9)	O(4)−Eu−O(6)#1	128.14(9)	O(4)−Eu−O(7)	79.51(9)
O(5)−Eu−O(6)	112.32(9)	O(5)−Eu−O(6)#1	52.08(9)	O(5)−Eu−O(7)	72.77(11)
O(6)−Eu−O(6)#1	65.60(10)	O(6)−Eu−O(7)	71.31(9)	O(6)#1−Eu−O(7)	78.21(10)

4[d]

Tb−O(1)	2.425(2)	Tb−O(2)	2.351(3)	Tb−O(2)#1	2.561(3)
Tb−O(3)	2.343(3)	Tb−O(4)	2.420(4)	Tb−O(5)	2.467(3)
Tb−O(5)#2	2.480(3)	Tb−O(6)	2.469(2)	Tb−O(7)	2.416(3)
O(1)−Tb−O(2)	123.16(9)	O(1)−Tb−O(2)#1	51.66(9)	O(1)−Tb−O(3)	78.24(10)
O(1)−Tb−O(4)	100.14(11)	O(1)−Tb−O(5)	75.98(9)	O(1)−Tb−O(5)#2	139.30(9)
O(1)−Tb−O(6)	143.74(10)	O(1)−Tb−O(7)	77.13(10)	O(2)−Tb−O(2)#1	72.46(10)
O(2)−Tb−O(3)	74.83(10)	O(2)−Tb−O(4)	70.84(10)	O(2)−Tb−O(5)	140.69(9)
O(2)−Tb−O(5)#2	95.75(9)	O(2)−Tb−O(6)	73.79(10)	O(2)−Tb−O(7)	141.50(10)
O(2)#1−Tb−O(3)	71.48(9)	O(2)#1−Tb−O(4)	74.63(10)	O(2)#1−Tb−O(5)	109.49(9)
O(2)#1−Tb−O(5)#2	154.62(9)	O(2)#1−Tb−O(6)	138.09(9)	O(2)#1−Tb−O(7)	124.35(9)
O(3)−Tb−O(4)	137.37(9)	O(3)−Tb−O(5)	144.21(9)	O(3)−Tb−O(5)#2	128.16(9)
O(3)−Tb−O(6)	76.31(10)	O(3)−Tb−O(7)	78.92(10)	O(4)−Tb−O(5)	72.08(9)
O(4)−Tb−O(5)#2	80.30(10)	O(4)−Tb−O(6)	116.07(10)	O(4)−Tb−O(7)	142.96(10)
O(5)−Tb−O(5)#1	65.37(10)	O(5)−Tb−O(6)	112.34(10)	O(5)−Tb−O(7)	71.46(10)
O(5)#2−Tb−O(6)	52.50(9)	O(5)#2−Tb−O(7)	78.92(10)	O(6)−Tb−O(7)	72.98(10)

5[e]

Yb−O(1)	2.311(11)	Yb−O(2)	2.464(11)	Yb−O(2)#1	2.247(10)
Yb−O(3)	2.465(12)	Yb−O(3)#2	2.240(10)	Yb−O(4)	2.327(11)
Yb−O(5)	2.137(12)	Yb−O(7)	2.256(12)		

Table 2 (Continued)

			5[e]		
O(1)−Yb−O(2)	53.4(4)	O(1)−Yb−O(2)#1	121.2(4)	O(1)−Yb−O(3)	144.8(4)
O(1)−Yb−O(3)#2	83.5(4)	O(1)−Yb−O(4)	147.5(4)	O(1)−Yb−O(5)	78.8(4)
O(1)−Yb−O(7)	81.2(4)	O(2)−Yb−O(2)#1	67.9(4)	O(2)−Yb−O(3)	139.5(4)
O(2)−Yb−O(3)#2	83.9(4)	O(2)−Yb−O(4)	140.0(4)	O(2)−Yb−O(5)	132.1(4)
O(2)−Yb−O(7)	81.4(4)	O(2)#1−Yb−O(3)	81.4(4)	O(2)#1−Yb−O(4)	81.7(4)
O(2)#1−Yb−O(3)#2	89.0(4)	O(2)#1−Yb−O(5)	159.5(4)	O(2)#1−Yb−O(7)	92.9(4)
O(3)−Yb−O(3)#2	69.3(4)	O(3)−Yb−O(4)	53.0(3)	O(3)−Yb−O(5)	78.8(4)
O(3)−Yb−O(7)	127.5(4)	O(3)#2−Yb−O(4)	122.3(4)	O(3)#2−Yb−O(5)	88.9(5)
O(3)#2−Yb−O(7)	163.2(4)	O(4)−Yb−O(5)	82.1(5)	O(4)−Yb−O(7)	74.5(4)
O(5)−Yb−O(7)	94.9(5)				

[a] Symmetry transformations used to generate equivalent atoms. #1: $-x+2, -y+2, -z+1$. #2: $-x+1, -y+2, -z+1$. [b] Symmetry transformations used to generate equivalent atoms. #1: $-x+1, -y+2, -z$. #2: $-x, -y+2, -z$. [c] Symmetry transformations used to generate equivalent atoms. #1: $-x, -y, -z+1$. #2: $-x+1, -y, -z+1$. [d] #1: $-x+1, -y, -z+1$. #2: $-x, -y, -z+1$. [e] #1: $-x+1, -y, -z+1$. #2: $-x, -y, -z+1$.

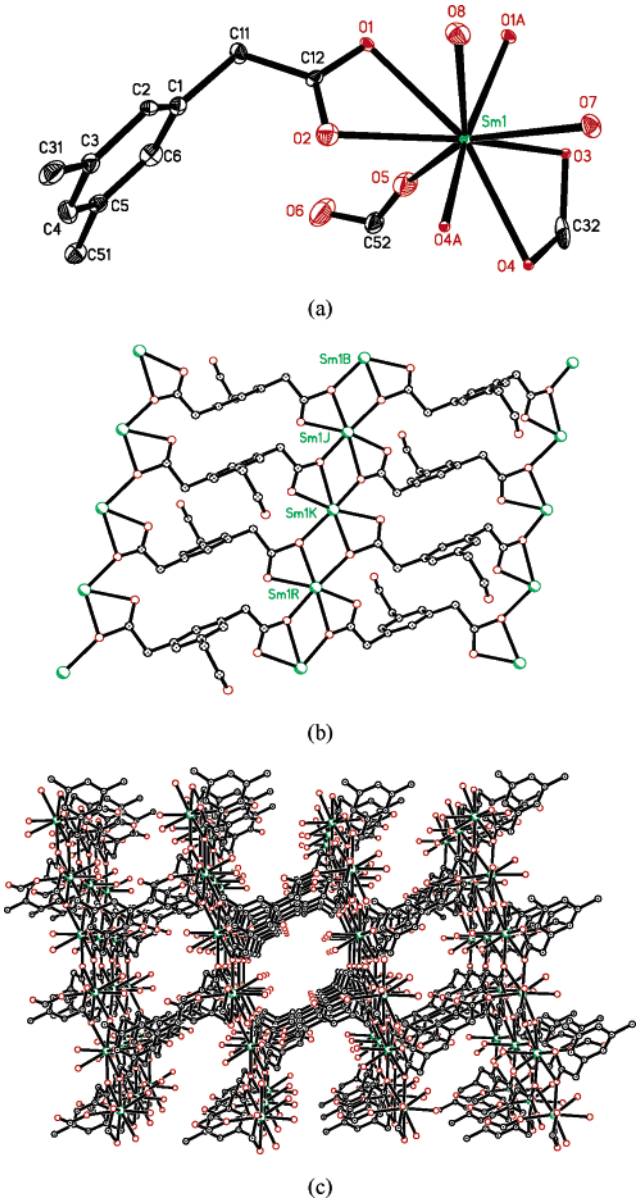

Figure 1. (a) ORTEP plot of **2** showing the local coordination environment of Sm^{III} with thermal ellipsoids at 30% probability. (b) The 2D network structure in **2**; water molecules are omitted for clarity. (c) Packing diagram of **2** along the *c* axis. Guest water molecules are omitted for clarity.

Scheme 1

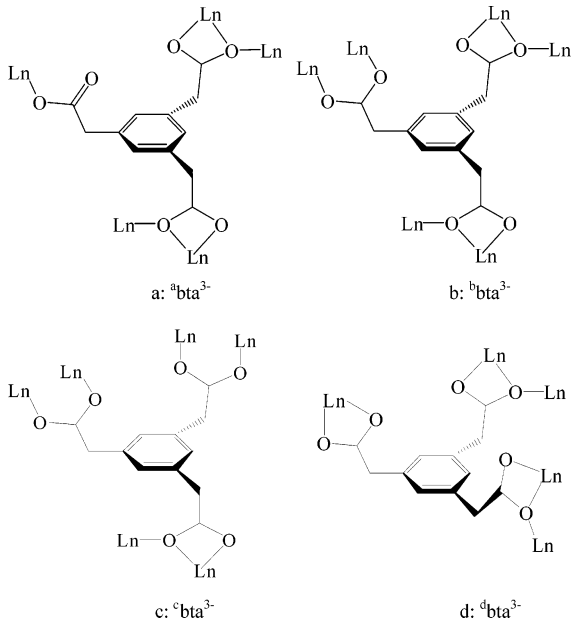

$[Eu(bta)(H_2O)\cdot 1.48H_2O]_n$ (3) and $[Tb(bta)(H_2O)\cdot 1.31H_2O]_n$ (4). The same space group and similar cell parameters for these complexes, as listed in Table 1, indicate that complexes **3** and **4** are isostructural, and hence, only the structure of complex **3** will be described here in detail. Each Eu^{III} ion is surrounded by nine O atoms provided by six bta^{3-} anions and one aqua molecule to form a distorted tricapped trigonal prism (Figure 2a). The Eu−O distances range from 2.370(3) to 2.571(3) Å, and the coordination angles vary from 51.53(9)° to 154.52(10)° (Table 2). In this complex, all carboxyl groups of the H_3bta are deprotonated, in good agreement with the IR spectral data since no strong bands around 1702 cm^{-1} for −COOH were observed. The C−O distances of the deprotonated carboxylate groups are typical, in the range of 1.249(4)−1.285(5) Å. Each bta^{3-} ligand adopts a cis, trans, trans conformation to link six europium(III) atoms, and three carboxylate groups of each bta^{3-} ligand also adopt two different coordination modes in **3** but different from those in complexes **1** and **2**, as schematically shown in Scheme 1b. One carboxylate group adopts a μ_2-η^1:η^1-bridging (each O atom coordinates to one metal atom, and the carboxylate group coordinates to two metal atoms) mode, while each of the other two carboxylate groups adopts a μ_2-η^2:η^1-bridging coordination mode. If we neglect the bridging functions of O3 and O4 (as shown in Figure 2a) in the μ_2-η^1:η^1-bridging carboxylate groups of $^b bta^{3-}$, each bta ligand links four Eu^{III} centers and each Eu^{III}

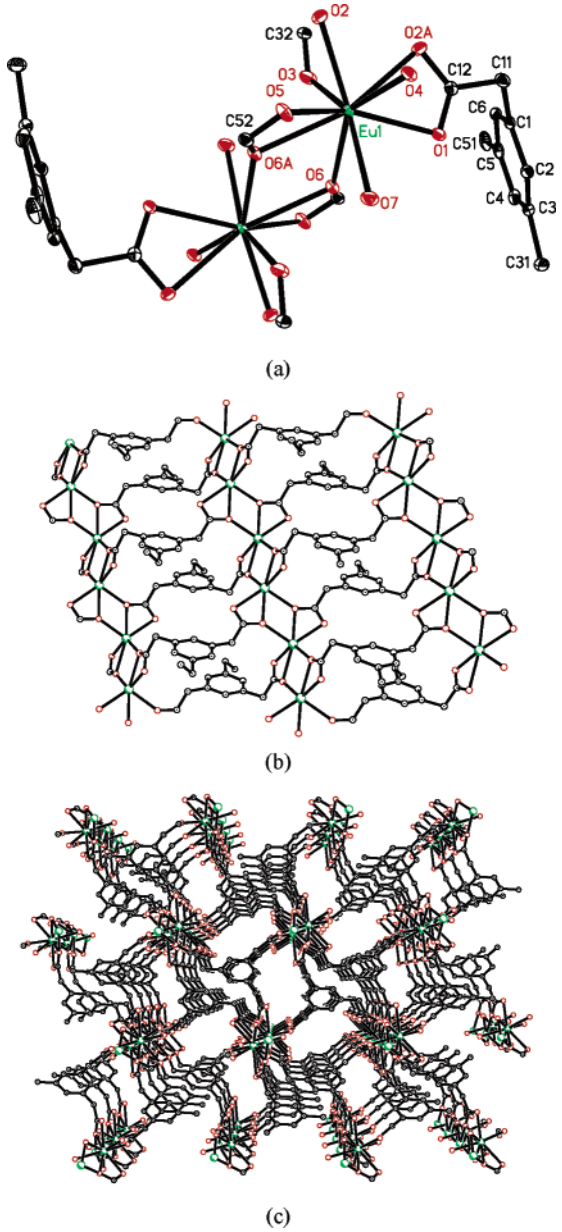

Figure 2. (a) ORTEP plot of **3** showing the local coordination environment of Eu^{III} with thermal ellipsoids at 30% probability. (b) The 2D network structure in **3**; water molecules are omitted for clarity. (c) The 3D structure viewed along the *a* axis of **3**. Guest water molecules are omitted for clarity.

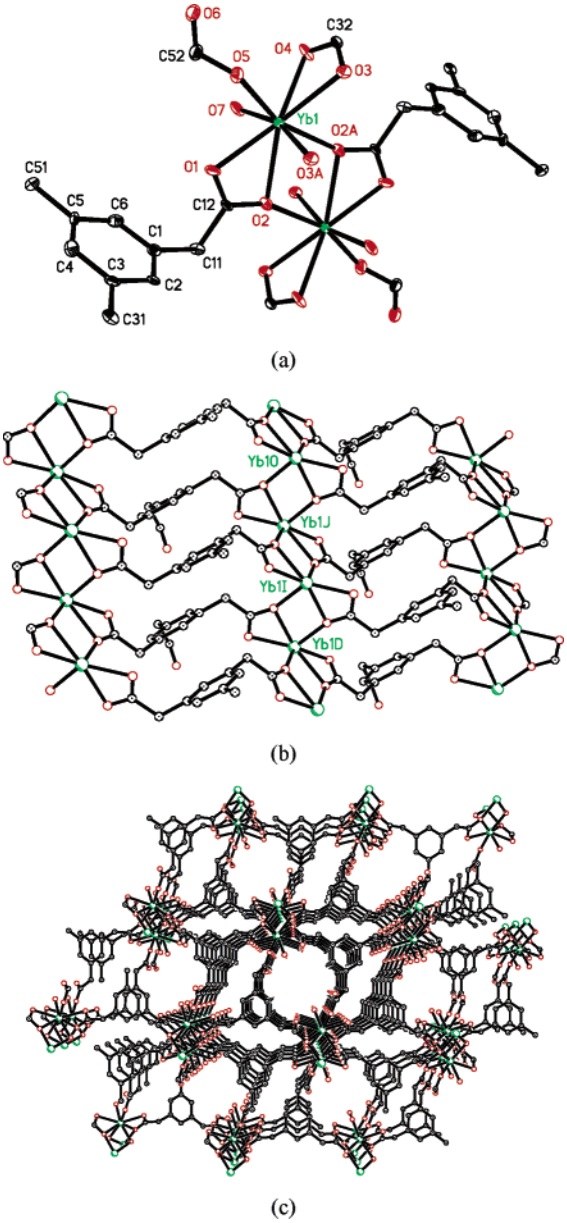

Figure 3. (a) ORTEP plot of **5** showing the local coordination environment of Yb^{III} with thermal ellipsoids at 30% probability. (b) The zigzag-like network structure of **5**; water molecules are omitted for clarity. (c) The 3D structure along the *a* axis of **5**. Guest water molecules are omitted for clarity.

center coordinates to four bta^{3-} ligands to form a 2D network with the nearest metal−metal distance of 3.991(1) Å (Figure 2b). In this 2D network, the Eu^{III} atoms and μ_2-η^2:η^1-bridging O atoms form an infinite zigzag chain, and these chains are bridged by a bta^{3-} ligand to generate the soft ladders, which are formed by using the chains as sharing sidepieces and the bta ligands as rungs. Then the 2D networks are further linked by the μ_2-η^1:η^1-bridging carboxylate groups, to generate a novel 3D open framework structure with channels along the *a* axis (Figure 2c), and the voids of the channels are occupied by the uncoordinated water molecules (Figure S2, Supporting Information).

$[Yb(bta)(H_2O)\cdot H_2O]_n$ (5). In the crystal structure of **5**, there are eight O atoms coordinated to the Yb^{III} ion with a trigonal dodecahedron coordination geometry, as illustrated in Figure 3a, seven of which come from five bta^{3-} ligands, and the additional one is from the coordinated water molecule. The Yb−O bond distances range from 2.137(12) to 2.465(12) Å, which are similar to other related Yb−O distances,[12] and the coordination angles vary from 53.0(3)° to 159.5(4)°, as listed in Table 2. Similar to complexes **1**−**4**, all three carboxyl groups of bta in **5** are deprotonated and the C−O distances of the deprotonated carboxylic groups are typical, falling in the range from 1.227(19) to 1.270(19) Å. There are also two coordination types of the carboxylate group of the bta^{3-} ligand in **5** similar to those observed in complexes **1** and **2**. If the linking functions of the monodentate carboxylate groups in $^a bta^{3-}$ are neglected, each

(12) (a) Wu, L. P.; Munakata, M.; Kuroda-Sowa, T.; Maekawa, M.; Suenaga, Y. *Inorg. Chim. Acta* **1996**, *249*, 183. (b) Ishikawa, N.; Iino, T.; Kaizu, Y. *J. Am. Chem. Soc.* **2002**, *124*, 11440.

ligand links four Yb^{III} atoms to form a 2D network with infinite zigzag Yb−O chains (for example, ∠Yb1O−Yb1J−Yb1I = ∠Yb1J−Yb1I−Yb1D = 101.9°; Figure 3b). The networks are further linked together by the monodentate coordinated carboxylate groups, to generate a 3D structure containing channels along the *a* axis (Figure 3c), which are filled by guest water molecules (Figure S3, Supporting Information).

Comparison of the Structures. The rigid ligands with the carboxylate groups attached to the central aromatic rings directly, such as 1,3,5-benzenetricarboxylic acid (H_3btc), 1,4-benzenedicarboxylic acid (*p*-H_2bdc), 1,3-benzenedicarboxylic acid (*m*-H_2bdc), and 1,2,4,5-benzenetetracarboxylic acid (H_4-btec), have been used extensively in the construction of coordination polymers.[3] In contrast to these rigid ligands with little or no conformational changes when they interact with metal salts, the flexible ligands have many more conformation and coordination modes. Accordingly, we selected a flexible tripodal ligand, H_3bta, which has a methylene group between each carboxylate group and the central benzene ring group, to assemble into coordination polymers with various metal salts.

The results show that there are different conformations and plentiful coordination modes for the bta^{3-} ligand in its metal complexes. Compared to the transition or alkaline earth metal complexes of bta^{3-},[4] for example, in $Co(Hbta)(H_2O)_4$ and $Ni(Hbta)(H_2O)_4$, each bta^{3-} ligand has a cis, trans, trans conformation, in which one carboxylate group without deprotonation remains free of coordination while each of the other two carboxylate groups adopts a μ_1-η^1:η^0-monodentate coordination mode to connect the metal ion.[4a] However, in the case of $[Ca_3(bta)_2(H_2O)_8]\cdot 3H_2O$, each bta^{3-} ligand with a cis, cis, cis conformation binds to five calcium atoms with one carboxylate group adopting a μ_3-η^2:η^2-bridging coordination mode, one a μ_2-η^2:η^1-bridging mode, and the third remaining uncoordinated with the metal atom. In $Ba_3(bta)_2(H_2O)_8$, each bta^{3-} ligand also binds to five metal atoms with a cis, cis, cis conformation, but the carboxylic groups adopt μ_3-η^2:η^2-bridging and μ_3-η^2:η^1-bridging coordination modes.[4b] In the above complexes, only two of three carboxylate groups of the bta^{3-} ligand apply to link the metal atoms. However, in recently reported complexes[5] and the title complexes, all the carboxylate groups are participating in the coordination with lanthanide metal atoms. In $[La(bta)(H_2O)_2]\cdot 4.5H_2O$,[5] **1**, **2**, and **5**, each bta^{3-} ligand adopts a cis, trans, trans conformation and acts as a μ_5 bridge to link five metal atoms (Scheme 1a), and in the previously reported complex $[Pr_2(bta)_2(H_2O)_3]\cdot 2H_2O$,[5] the bta^{3-} ligands adopt cis, trans, trans and cis, cis, cis conformations and act as μ_6 and μ_5 bridges (Scheme 1c and d), respectively. However, in complexes **3** and **4**, the bta^{3-} ligands adopt a cis, trans, trans conformation and act as μ_6 bridges (Scheme 1b). Such a difference in the coordination modes of bta^{3-} between the lanthanide and transition metal as well as alkaline earth metal complexes can be attributed to the large radii and positive charge of the Ln^{III} ions, and hence, the bta^{3-} anions tend to adopt different conformations and more varied coordination modes to saturate their higher coordination numbers.

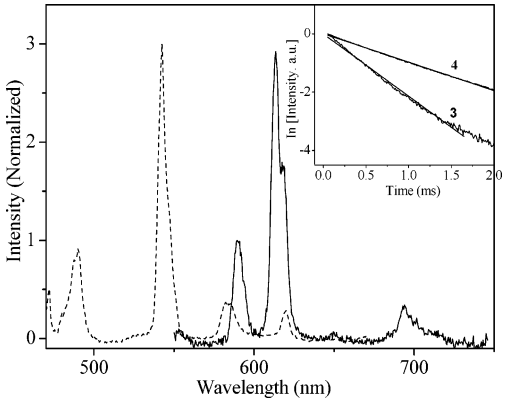

Figure 4. Photoluminescence spectra of complexes **3** (solid line) and **4** (dash line) in the solid state at ambient temperature. Inset: Luminescence decay curves for **3** and **4** at ambient temperature. The solid lines are the best fits of experimental data.

Table 3. Average Bond Lengths and the Coordination Numbers (CN) in **1**−**5**

		average bond length/Å	
complex	CN	$Ln-O_{carboxylate}$	$Ln-O_w$ (water)
1	9	2.499	2.499
2	9	2.457	2.475
3	9	2.463	2.447
4	9	2.440	2.416
5	8	2.313	2.256

In complexes **1** and **2**, the average bond length of $Ln-O_{carboxylate}$ is similar or shorter than that of $Ln-O_w$ (water), while in complexes **3**−**5**, the average bond length of $Ln-O_{carboxylate}$ is longer than that of $Ln-O_w$, and the coordination numbers (CN) of the Ln^{III} ions are varied from 9 (Nd^{III}, Sm^{III}, Eu^{III}, and Tb^{III}) to 8 (Yb^{III}), as shown in Table 3. This is probably caused by the change of coordination mode and the lanthanide contraction effect in the series on the whole. Especially, in complexes **1**, **2**, and **5**, the bta^{3-} ligands adopt the same conformation and coordination modes, but because of the different coordination numbers of the center metal ions and different bond angles of ∠O−Ln−O, three complexes showed two different kinds of structures, as described above.

Photoluminescent Properties. Lanthanide luminescence is demonstrated to be very sensitive to the local environments around the lanthanide center.[13] When the Eu^{III} complex **3** was excited at 394 nm, characteristic luminescent bands were recorded at 590, 614, 648, and 694 nm via the ligand-to-metal energy transfer mechanism, which correspond to the transitions from the $^5D_0$ state to the ^7F_n (n = 1−4) levels, respectively.[14] The luminescent spectrum of complex **3**, which was normalized with respect to the $^5D_0 \rightarrow {}^7F_1$ (magnetic dipole) transition at 590 nm, was illustrated in Figure 4. It is noted that the intensity ratio of the $^5D_0 \rightarrow {}^7F_2$

(13) (a) Foster, D. R.; Richardson, F. S. *Inorg. Chem.* **1983**, *22*, 3996. (b) Yanagida, S.; Hasegawa, Y.; Murakoshi, K.; Wada, Y.; Nakashima, N.; Yamanaka, T. *Coord. Chem. Rev.* **1998**, *171*, 461. (c) Yamada, T.; Shinoda, S.; Sugimoto, H.; Uenishi, J.-i.; Tsukube, H. *Inorg. Chem.* **2003**, *42*, 7932.

(14) (a) Buono-Core, G. E.; Li, H. *Coord. Chem. Rev.* **1990**, *99*, 55. (b) Taki, M.; Murakami, H.; Sisido, M. *Chem. Commun.* **2000**, 1199. (c) Montalti, M.; Prodi, L.; Zaccheroni, N.; Charbonniere, L.; Douce, L.; Ziessel, R. *J. Am. Chem. Soc.* **2001**, *123*, 12694.

transition to the $^5D_0 \rightarrow {}^7F_1$ transition is widely used as a measure of the coordination state and the site symmetry of the europium ion, since the $^5D_0 \rightarrow {}^7F_1$ emission is relatively strong, independent of the ligand environment, and primarily magnetic dipole in character, while the $^5D_0 \rightarrow {}^7F_2$ emission is essentially purely electric dipole in character, and its intensity is very sensitive to the crystal field symmetry. Among the $^5D_0 \rightarrow {}^7F_J$ transitions, only $^5D_0 \rightarrow {}^7F_1$ satisfies the $\Delta J = 0, \pm 1$ (excluding $J = J' = 0$) intermediate-coupling selection rule for magnetic dipole intensity, so its intensity is predicted to be primarily magnetic dipole in nature and only weakly dependent on crystal field effects. The remaining transitions can acquire magnetic dipole intensity only via crystal-field-induced *J*-level mixing. At first order in the odd-parity components of the crystal field potential, only the $^5D_0 \rightarrow {}^7F_{2,4,6}$ transitions are predicted to be electric-dipole-allowed in the absence of *J*-level mixing and its intensity is strongly dependent on the odd-parity components of the crystal field, while the $^5D_0 \rightarrow {}^7F_{0,1,3,5}$ transitions cannot acquire electric dipole intensity until *at least* second order—first order in the odd-parity crystal field components and first order in the even-parity crystal field components (the latter being responsible for *J*-level mixing).[15] In complex **3**, the $^5D_0 \rightarrow {}^7F_2$ transition is the strongest one in the four transitions, with about three times the strength of the transition of $^5D_0 \rightarrow {}^7F_1$. The results show that Eu^{III} has the lower symmetric coordination environment close to a D_2 symmetry in **3**.[16] This is consistent with the result of the single-crystal X-ray analysis.

For complex **3**, the experimental luminescent decay curve fits well with single exponential decay, and the lifetime of 0.45 ms is obtained (Figure 4). Vibrations of water molecules can effectively remove the electronic energy of excited europium ions, and the hydration number (*n*) in crystalline Eu^{III} complexes can be estimated from the lifetime, τ in ms, by using the equation $n = 1.05\tau^{-1} - 0.70$.[17] The hydration number of **3** was calculated to be 1.63 despite the fact that **3** has one distinct Eu site [$EuO_8(H_2O)$]. This may be attributable to the effective coupling between Eu^{III} ions as well as the participation of water molecules in the outer coordination sphere.[18]

When the Tb complex **4** was excited at 370 nm, it gave a typical Tb^{III} emission spectrum containing the expected sequence of $^5D_4 \rightarrow {}^7F_J$ ($J = 6 - 3$) transitions (Figure 4). The spectrum is dominated by the $^5D_4 \rightarrow {}^7F_5$ transition, at 542 nm, which gives an intense green luminescence output for the solid sample. The lifetime of complex **2** is 1.0 ms,

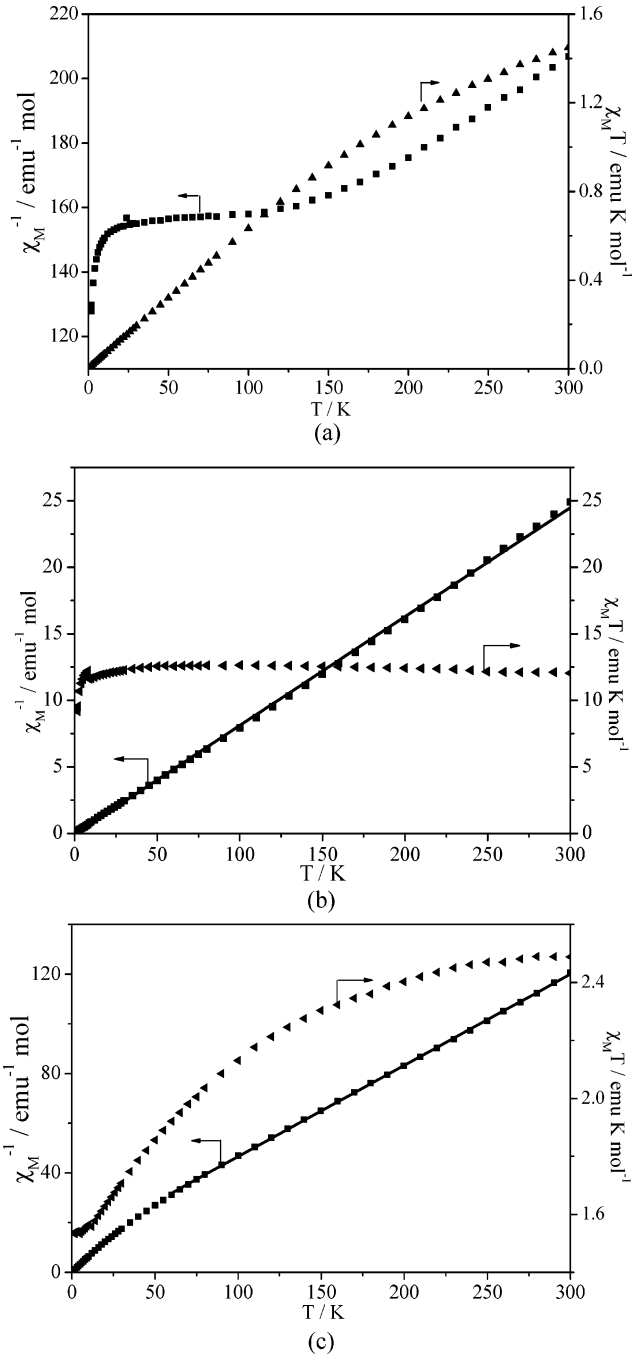

Figure 5. Plots of the temperature dependencies of χ_MT (▲) and χ_M^{-1} (■) for complexes **3** (a), **4** (b), and **5** (c); the solid line represents the best fit of the curve.

and its experimental curve also fits well with single-exponential decay (Figure 4) at ambient temperatures.

Magnetic Properties. The difficulty in studying the magnetic properties of species containing paramagnetic Ln^{III} ions arises from the fact that most of the Ln^{III} ions possess a first-order angular momentum. For the $4f^n$ configuration of a Ln^{III} ion, it splits into $^{2S+1}L_J$ states by interelectronic repulsion and spin−orbit coupling.[7,19] Further splitting into Stark sublevels is caused by crystal-field perturbation. At

(15) (a) Kirby, A. F.; Foster, D.; Richardson, F. S. *Chem. Phys. Lett.* **1983**, *95*, 507. (b) Xu, Q. H.; Li, L. S.; Liu, X. S.; Xu, R. R. *Chem. Mater.* **2002**, *14*, 549. (c) Kim, Y. J.; Suh, M.; Jung, D. Y. *Inorg. Chem.* **2004**, *43*, 245.

(16) (a) Horrocks, W. W., Jr.; Sudnick, D. R. *Acc. Chem. Res.* **1981**, *14*, 384. (b) Bartelemy, P. P.; Choppin, G. R. *Inorg. Chem.* **1989**, *28*, 3354. (c) Choppin, G. R.; Peterman, D. R. *Coord. Chem. Rev.* **1998**, *174*, 283.

(17) Dickins, R. S.; Parker, D.; Sousa, A. S.; Williams, J. A. G. *Chem. Commun.* **1996**, 697.

(18) (a) Kirby, A. F.; Richardson, F. S. *J. Phys. Chem.* **1983**, *87*, 2544. (b) Murray, G. M.; Sarrio, R. V.; Peterson, J. R. *Inorg. Chim. Acta* **1990**, *176*, 233.

(19) (a) Kahn, M. L.; Ballou, R.; Porcher, P.; Kahn, O.; Sutter, J.-P. *Chem. Eur. J.* **2002**, *8*, 525. (b) Costes, J.-P.; Nicodème, F. *Chem. Eur. J.* **2002**, *8*, 3442.

room temperature, all the Stark levels are populated, but as the temperature decreases, the effective magnetic moment of the lanthanide ion will change by thermal depopulation of the Stark sublevels, even for a mononuclear Ln^{III} complex; the temperature dependence causes the magnetic susceptibility to deviate from the Curie behavior. This phenomenon is intrinsic to the lanthanide ion and is modulated by the ligand field and the symmetry of the compound.[7,19]

The temperature dependence of the magnetic susceptibility of complex **3** is shown in Figure 5a, where χ_M is the corrected molar magnetic susceptibility per Eu^{III} ion. The observed $\chi_M T$ at room temperature is 1.45 emu K mol^{-1}, slightly less than the value of 1.5 for a Eu^{III} ion calculated from the Van Vleck equation allowing for population of the lower excited state with higher values of J at 293 K. As the temperature is lowered, $\chi_M T$ decreases continuously as a result of the depopulation of the Stark levels for a single Eu^{III} ion. At the lowest temperature, $\chi_M T$ is close to zero, indicating a $J = 0$ ground state of the Eu^{III} ion ($^7F_0$). The magnetic susceptibility above 150 K follows the Curie−Weiss law because of the presence of thermally populated excited states.[20]

The magnetic behavior of complex **4** is shown in Figure 5b as the thermal variation of the $\chi_M T$ versus T plot, where χ_M is the corrected molar magnetic susceptibility per [Tb] unit. The $\chi_M T$ product is practically constant over the entire temperature range with an observed value (12.05 emu K mol^{-1} at room temperature) corresponding to a free Tb^{III} ion (11.82 emu K mol^{-1}) according to the structure, and the plot of χ_M^{-1} versus T over the whole temperature range obeys the Curie−Weiss law with $C = 12.23$ emu mol^{-1} K and $\theta = 0.83$ K. All these finding indicate that the intra- and intermolecular Tb−Tb magnetic interactions are very weak.

For complex **5**, the observed value of $\chi_M T$ per [Yb] unit is 2.49 emu K mol^{-1} at room temperature (Figure 5c), which is close to the calculated value (2.57 emu K mol^{-1}) for a free Yb^{III} ion. The value of $\chi_M T$ decreases slowly as the temperature decreases, to reach a value of 1.53 emu K mol^{-1} at 1.8 K. The plot of χ_M^{-1} versus T over the temperature range 60−300 K obeys the Curie−Weiss law with $C = 2.74$ emu K mol^{-1} and $\theta = -28.32$ K. The decrease of $\chi_M T$ and the negative value of θ are due primarily to the splitting of the ligand field of the Yb^{III} ion together with the possible weak antiferromagnetic coupling between the Yb^{III} ions, considering a possible interaction path through carboxylate bridges with a 3.911(4) Å Yb−Yb distance.

Acknowledgment. This work was supported by the National Natural Science Foundation of China (Grant 20231020) and the National Science Fund for Distinguished Young Scholars (Grant 20425101).

Supporting Information Available: X-ray crystallographic file in CIF format and crystal packing diagram for **2**, **3**, and **5** (Figures S1, S2, and S3, respectively). This material is available free of charge via Internet at http://pubs.acs.org.

IC050453A

(20) (a) Wan, Y. H.; Zhang, L. P.; Jin, L. P.; Gao, S.; Lu, S. Z. *Inorg. Chem.* **2003**, *42*, 4985. (b) Zheng, X. J.; Sun, C. Y.; Lu, S. Z.; Liao, F. H.; Gao, S.; Jin, L. P. *Eur. J. Inorg. Chem.* **2004**, 3262.